Evaluation Of The Need For Discontinuity Factors For Neutronic Modelling Of CANDU® Low-Void Reactivity Fuel Lattices

E. Nichita

School of Energy Systems and Nuclear Science
University of Ontario Institute of Technology
2000 Simcoe Street North
Oshawa, ON L1H 7K4
eleodor.nichita@uoit.ca

Abstract

The need for and effectiveness of using assembly discontinuity factors (ADFs) in neutronic diffusion calculations for low-void-reactivity fuel (LVRF) CANDU lattices was investigated. Two simple configurations were used for this purpose: one consisting of two adjacent fuel cells with different burnups and one consisting of two fuel cells and one reflector cell. Diffusion calculations were performed in two energy groups using homogenized nodes. Four discretization methods were used: Coarse-Mesh Finite Differences (CMFD), Fine-Mesh Finite Differences (FMFD), Nodal Expansion Method (NEM) without ADFs and NEM with ADFs. The diffuson results were then compared with reference results obtained from 69-energy-group transport calculations using detailed geometrical representations. It was found that using (zero-crrent) ADFs results in minimal improvement of acuracy and that a better (leakage corrected) homogenization method is neded to further increase accuracy.

1 INTRODUCTION

Full-core neutronic calculations are usually carried out in diffusion theory, using fuel-bundle-size homogenized nodes. The homogenized macroscopic cross sections are obtained by averaging the detailed-geometry macroscopic cross sections. Finding adequate homogeneous parameters is the topic of Equivalence Theory (ET), which was originally developed by Koebke[1], and later extended by Smith[2,3] under the name of Generalized Equivalence Theory (GET).

In the context of GET, the detailed geometric core model is called the *heterogeneous* model, while the simplified, homogeneous-node model is called simply the *homogeneous* model. Likewise, the detailed flux is called the *heterogeneous* flux, while the flux obtained for the homogeneous model is called the *homogeneous* flux.

GET offers a method to find homogeneous parameters for each node, so that the node-integrated reaction rates of the homogeneous model are the same as those for the heterogeneous model. GET shows that to obtain identical node-integrated reaction rates in the heterogeneous and homogeneous nodes the homogeneous multigroup flux has to be only piecewise continuous; that is continuous in each homogeneous node, but discontinuous at node boundaries. At the interface *s* between two nodes i and j, a "discontinuity" condition is written:

$$\overline{\Phi}_{sg}^{i} f_{sg}^{i} = \overline{\Phi}_{sg}^{j} f_{sg}^{j} \tag{1}$$

where $\overline{\Phi}_{sg}^{i}$ and $\overline{\Phi}_{sg}^{j}$ are the homogeneous fluxes in nodes i and j respectively, averaged over the common face. Factors f_{sg}^{i} and f_{sg}^{j} are called *discontinuity factors*, and are defined as the ratio of the face-averaged heterogeneous flux Ψ to the face-averaged homogeneous flux Φ:

$$f_{sg} \equiv \frac{\overline{\Psi}_{sg}}{\overline{\Phi}_{sg}} \tag{2}$$

The homogeneous cross sections are given, according to GET, by the simple flux-weighted volume-averaged-values:

$$\hat{\Sigma}_{g} \equiv \frac{\int_{V} \Sigma_{g}(\vec{r}) \Psi_{g}(\vec{r}) d^{3}r}{\int_{V} \Psi_{g}(\vec{r}) d^{3}r} \tag{3}$$

The discontinuity of the face-averaged homogeneous flux expressed by Eq. (1) represents the continuity of the face-averaged heterogeneous flux across the node interface. If the discontinuity factors in adjacent nodes are equal, Eq. (1) reduces to the regular continuity condition for the face-averaged homogeneous flux:

$$\overline{\Phi}_{sg}^{i} = \overline{\Phi}_{sg}^{j} \tag{4}$$

Hence, if two adjacent nodes have discontinuity factors of almost equal value, the use of discontinuity factors is unnecessary. The use of discontinuity factors is only important at interfaces separating dissimilar nodes (i.e. with considerably different discontinuity factors).

The definition of the discontinuity factors contained in Eq. (2) is mathematically correct, but requires the homogeneous flux to be known beforehand. To avoid the above-mentioned difficulty, approximate discontinuity factors are calculated using reflective boundary conditions on the heterogeneous node boundary. Zero-current discontinuity factors are also called Assembly Discontinuity Factors (ADFs), because in

light-water reactors a node usually corresponds to a fuel assembly. In CANDU reactors a node usually corresponds to a lattice cell. ADFs can be shown to be equal to the ratio between the face-averaged heterogeneous flux and the node-averaged heterogeneous flux[3].

$$f_{sg}^{0} = \frac{\overline{\Psi}_{Sg}^{0}}{\overline{\Psi}_{Vg}^{0}} \tag{5}$$

In Eq. (5) the "0" superscript signifies zero boundary current. It can also be shown that, for a homogeneous node for which the flux is separable in energy and space and for which the diffusion approximation is adequate, the discontinuity factors equal unity.

ADFs are a good approximation for most light-water-reactor configurations, but only limited experience exists for CANDU reactors[4]. The present work is devoted to assessing if ADFs are an effective tool for improving the accuracy of homogenized-node diffusion calculations for configurations involving LVRF nodes.

2 METHOD

To test the accuracy of diffusion calculations for LVRF nodes and the effect of ADFs, a two-node and a three-node configuration were used. The two-node configuration consists of a burnt (6000 KWd/Kg) fuel node and a fresh-fuel node. It is intended to offer an estimate of the achievable accuracy for nodes situated inside the core, far from the reflector. The three-node configuration consists of a burnt (6000 KWd/Kg) fuel node, a fresh fuel node and a reflector node, in that sequence. It is intended to offer an estimate of the achievable accuracy for nodes in the vicinity of the reflector. Reflective external boundary conditions were used for both configurations.

The reference (heterogeneous) calculations for each configuration were performed using the DRAGON[5] code (Rev. 3.04-S), in 69 energy groups (IAEA-WLUP library in WIMS-D format[6]), two dimensions, and with isotropic reflective boundary conditions. The NESTLE[7] (V5.2.1) code was used for the two-group (homogeneous) diffusion calculations. Several NESTLE calculations were performed for each of the two configurations:

- coarse-mesh (one mesh per node) finite difference (CMFD)
- fine-mesh (10 meshes per node) finite difference (FMFD)
- nodal expansion (NEM) without ADFs
- nodal expansion (NEM) with ADFs

The results of the NESTLE calculations were then compared with the results of the reference DRAGON calculations.

2.1. Fuel Bundle Parameters

Because the exact parameters for the LVRF bundles are not publicly available, generic parameters for a 43-element LVRF bundle were used, based loosely on published documents[8,9]. Some of those parameters are shown in Table 1.

TABLE 1: FUEL BUNDLE PARAMETERS

Fuel Density	10.6 g/cm^3
Fuel Temperature	1155 K
Central Element and First Ring Pin Outer Radius	0.675 cm
Central Element and First Ring Sheath Thickness	0.04 cm
Central Element and First Ring Fuel Pellet Radius	0.635 cm
Outer Two Rings Pin Outer Radius	0.575 cm
Outer Two Rings Sheath Thickness	0.04 cm
Outer Two Rings Fuel Pellet Radius	0.535 cm
Inner Ring Radius	1.6885 cm
Middle Ring Radius	3.0755 cm
Outer Ring Radius	4.5305 cm
Central Element Composition	8.8 % Dy in Natural U
First Ring Composition	1.9 % Dy in Natural U
Second Ring Composition	2.7 % Slightly Enriched U
Third Ring Composition	1.7 % Slightly Enriched U
Coolant	D_2O (99.75 % purity)
Moderator	D_2O (99.91 % purity)
Lattice Pitch	28.575 cm

2.2. Geometrical Models

The detailed modeling of a CANDU LVRF cell with DRAGON is shown in Figure 1. It is based on a fuel-pin "cluster" geometry. A true representation of two adjacent cells would comprise two fuel-pin clusters. Such an option was not yet available in DRAGON, so a simplified cell model was used, as shown in Figure 2. The simplified single-cell model was obtained from the detailed model by homogenizing the heavy water, clad and fuel in each fuel ring. The simplified single-cell model was used to generate cell-averaged parameters. The thin (1 mm) Cartesian regions on the boundary were used to find the boundary flux necessary for calculating the ADFs[10]. A detail of the lower left corner of the simplified-cell model is shown in Figure 3. The 2- and 3-cell simplified geometrical models are shown in Figures 4 and 5 respectively.

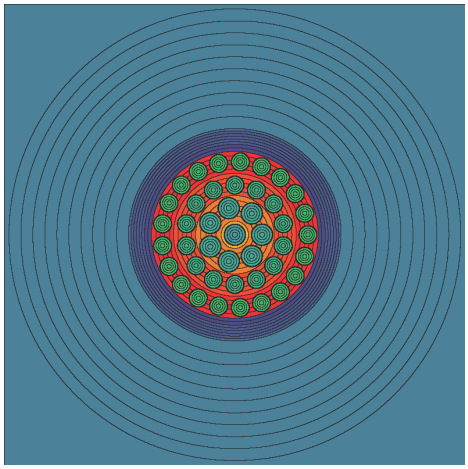

FIGURE 1: DETAILED SINGLE-FUEL-CELL DRAGON MODEL

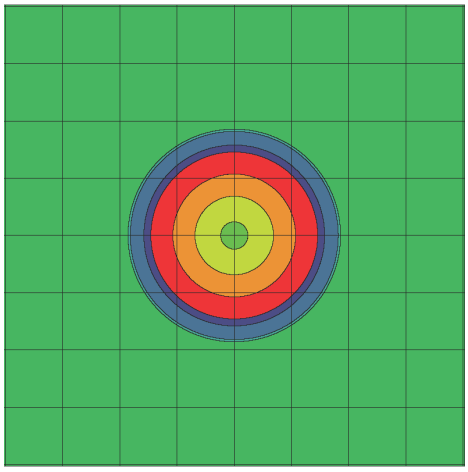

FIGURE 2: SIMPLIFIED SINGLE-FUEL-CELL DRAGON MODEL

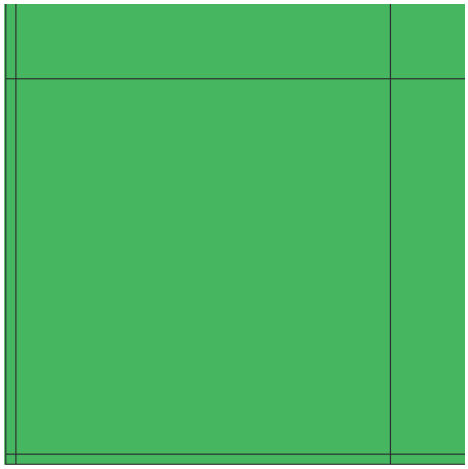

FIGURE 3: DETAIL OF THE CARTESIAN MESH FOR THE LOWER LEFT CORNER OF THE SIMPLIFIED MODEL

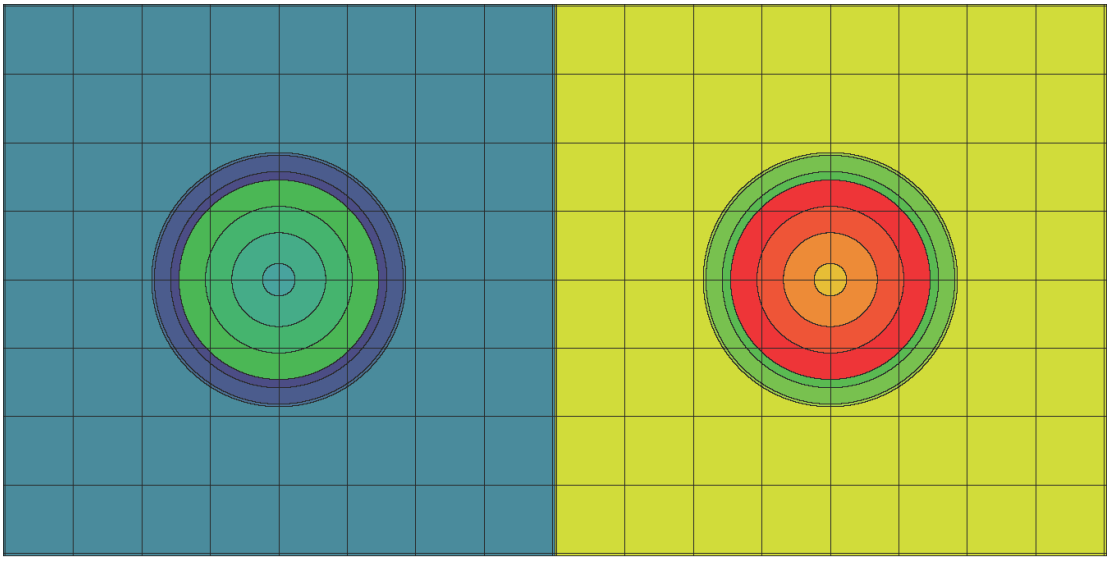

FIGURE 4: TWO-FUEL-CELL DRAGON MODEL

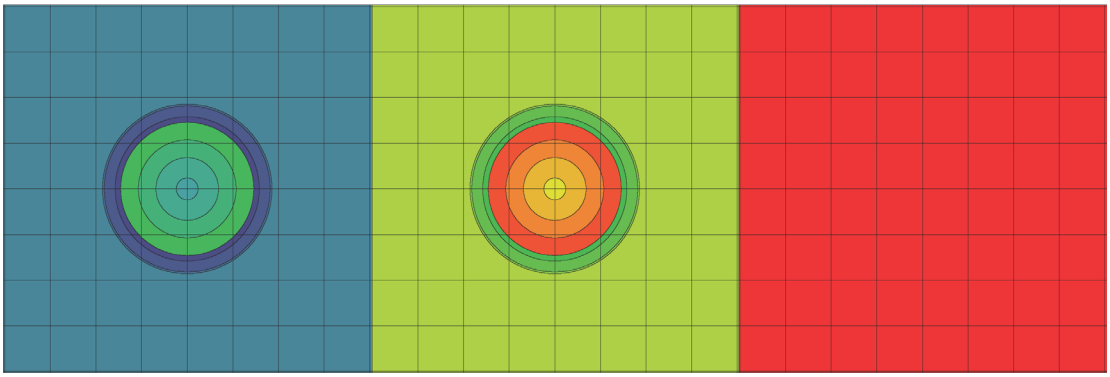

FIGURE 5: THREE-CELL (FUEL-FUEL-REFLECTOR) DRAGON MODEL

2.3. Generation of Node-Averaged Diffusion Cross Sections

Cell-averaged two-group macroscopic cross sections for the fuel nodes were generated using single-cell simplified-geometry DRAGON models with the appropriate burnup. The macroscopic cross sections for the reflector nodes were generated using a two-cell model consisting of a fresh-fuel cell adjacent to a reflector cell. The geometric model used for finding the reflector properties is shown in Figure 6. All calculations were performed with DRAGON in 69 energy groups, using isotropic reflective boundary conditions and zero buckling. The homogenized diffusion coefficients were calculated from the homogenized transport cross sections.

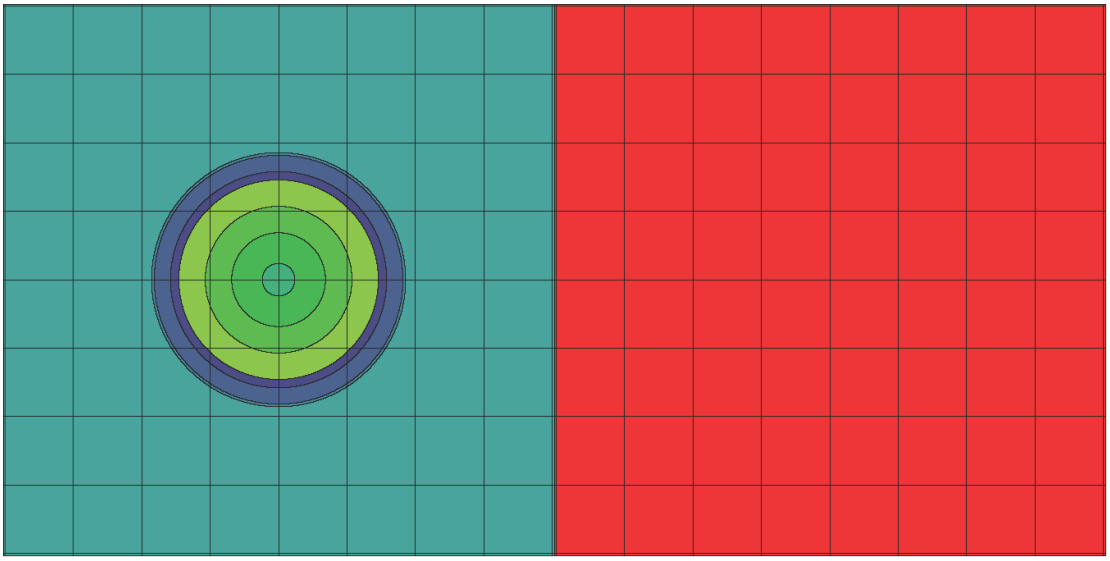

FIGURE 6: TWO-CELL DRAGON MODEL FOR GENERATING REFLECTOR CROSS SECTIONS

3 RESULTS

The values of the node-averaged two-group macroscopic cross sections and ADFs for the fuel nodes and the reflector node, are shown in Table 2.

Table 2: Node-Averaged Two-Group Macroscopic Cross Sections and ADFs

node	$k_{\inf}$	$\Sigma_{a1}(\text{cm}^{-1})$	$\Sigma_{a2}(\text{cm}^{-1})$	$\Sigma_{s12}(\text{cm}^{-1})$	$\Sigma_{s21}(\text{cm}^{-1})$	$\Sigma_{f1}(\text{cm}^{-1})$	$\Sigma_{f2}(\text{cm}^{-1})$
fresh	1.238916	0.002116	0.005638	0.008455	0.000099	0.000472	0.003254
burnt	1.132268	0.002162	0.005562	0.008403	0.000097	0.000405	0.002856
reflector		0.000004	0.000047	0.017713	0.000012	0.000000	0.000000
node	$k_{\inf}$			$\Sigma_{tr1}(\text{cm}^{-1})$	$\Sigma_{tr2}(\text{cm}^{-1})$	f_1	f_2
fresh	1.238916	0.001222	0.007935	0.252033	0.395803	0.818715	1.178967
burnt	1.132268	0.001068	0.007227	0.252217	0.395904	0.818121	1.176681
reflector		0.000000	0.000000	0.260486	0.418015	1.000000	1.000000

Table 2 shows that the values of the ADFs for the fresh and burnt fuel are very close (difference smaller than 1%). The use of ADFs is thus expected to have a negligible influence on the results for the two-fuel-node model.

The results for the two-fuel-node model are shown in Table 3. The results for the three-node model consisting of a burnt-fuel node, a fresh-fuel node and a reflector node are shown in Table 4. All results are normalized to an average volumetric fission rate of 1.

TABLE 3: TWO-FUEL-NODE MODEL RESULTS

Type of Calculation		K-eff	Fission Rate		Fast Flux		Thermal Flux	
			burnt	fresh	burnt	fresh	burnt	fresh
Transport (reference)		1.1872	0.905	1.095	189.623	213.104	290.697	305.097
CMFD	value	1.1891	0.875	1.125	184.443	217.426	280.096	314.285
	error	0.0019	-0.031	0.031	-5.180	4.322	-10.600	9.188
	% error	0.16	-3.39	2.80	-2.73	2.03	-3.65	3.01
FMFD	value	1.1880	0.895	1.105	189.687	212.720	286.681	308.538
	error	0.0008	-0.010	0.010	0.063	-0.384	-4.016	3.441
	% error	0.06	-1.08	0.89	0.03	-0.18	-1.38	1.13
NEM - w/o ADF	value	1.1880	0.896	1.104	189.743	212.663	286.737	308.490
	error	0.0007	-0.010	0.010	0.120	-0.441	-3.960	3.393
	% error	0.06	-1.06	0.88	0.06	-0.21	-1.36	1.11
NEM - w/ ADF	value	1.1879	0.896	1.104	189.875	212.564	286.978	308.276
	error	0.0007	-0.009	0.009	0.251	-0.540	-3.719	3.180
	% error	0.06	-0.98	0.81	0.13	-0.25	-1.28	1.04

TABLE 4: THREE-NODE (FUEL-FUEL-REFLECTOR) RESULTS

Type of Calculation		K-eff	Fission Rate		Fast Flux			Thermal Flux		
			burnt	fresh	burnt	fresh	reflector	burnt	fresh	reflector
Transport		1.19618	0.872	1.128	182.128	189.170	27.271	280.418	320.297	536.966
CMFD	value	1.19274	0.848	1.152	176.439	196.754	16.587	271.787	325.573	584.477
	error	-0.00344	-0.025	0.025	-5.689	7.584	-10.685	-8.630	5.276	47.511
	% error	-0.29	-2.86	2.21	-3.12	4.01	-39.18	-3.08	1.65	8.85
FMFD	value	1.20432	0.827	1.173	172.171	171.929	31.511	265.230	335.462	566.245
	error	0.00814	-0.045	0.045	-9.957	-17.242	4.240	-15.188	15.165	29.279
	% error	0.68	-5.20	4.02	-5.47	-9.11	15.55	-5.42	4.73	5.45
NEM w/o ADF	value	1.20462	0.826	1.174	172.046	171.350	31.863	264.921	335.833	565.683
	error	0.00844	-0.046	0.046	-10.082	-17.820	4.592	-15.497	15.536	28.717
	% error	0.71	-5.31	4.11	-5.54	-9.42	16.84	-5.53	4.85	5.35
NEM w/ ADF	value	1.20116	0.836	1.164	174.462	175.406	28.762	267.930	332.302	615.272
	error	0.00498	-0.037	0.037	-7.666	-13.764	1.491	-12.487	12.006	78.305
	% error	0.42	-4.21	3.26	-4.21	-7.28	5.47	-4.45	3.75	14.58

Table 3 shows that, for a pair of different-burnup bundles, the coarse-mesh results are less accurate than the FMFD and NEM results. It also shows that the FMFD, the NEM without ADFs and the NEM with ADFs all give virtually identical results. The fact that the NEM gives very close results to FMFD is a verification of the fact that NEM provides an accurate solution for the homogenized-node problem. The fact that the NEM with and without ADFs yields almost identical results is consistent with the fact that the ADFs of the two nodes are almost identical and hence make virtually no difference in the calculation. Consequently, no improvement in accuracy is gained from the use of ADFs. The absolute value of the percentage error of the fission rate is largest for the burnt-fuel node for all methods. It is approximately 3.5% for the CMFD method, 1.1% for the FMFD and NEM without ADF methods, and 1.0% for the NEM with ADFs. The

percentage errors in the fast and thermal flux display similar properties to the ones for the fission rate.

Table 4 shows that for a more demanding model, one including a reflector node, the results of the FMFD and NEM without ADFs are again quasi-identical but different from both the CMFD and NEM with ADFs. CMFD occupies the first place in accuracy, NEM with ADFs occupies the second place, while NEM without ADFs together with FMFD share the third place. The absolute value of the fission rate percentage error is, again, largest for the low-burnup node, for all methods. Its value is 2.9% for the CMFD method, 4.2 % for the NEM with ADFs and approximately 5.3 % for the FMFD and NEM without ADFs. The thermal flux percentage errors inside the fuel nodes have similar values to the ones for the fission rate. Interestingly, the minimum error is obtained using the CMFD method and not FMFD or NEM, as would be normally expected. This indicates that the homogenization process is an important contributor to the error.

4 CONCLUSION

The results in Table 3 and Table 4 show that, for LVRF lattices, the error in the CMFD diffusion calculations can be expected to be roughly between 2.5% and 3.5%. Using finer meshes or employing a more advanced method, such as NEM, yields to an increase in accuracy (error reduced to 1%) for nodes far from the reflector (Table 3), but yields to a significant decrease in accuracy (error increased to 4% - 5%) for the nodes neighboring the reflector. The use of ADFs leads to no improvement for the nodes inside the core and only marginal improvement for the nodes neighboring the reflector.

Since FMFD and nodal methods are very good at solving the homogenized-node models with high accuracy, and since they have been shown to give very close results to one another for both analyzed models, it can only be concluded that the remaining difference between the results of the diffusion calculations and those of the transport calculations is due to the inadequacy of the homogenized parameters (i.e. macroscopic cross sections and discontinuity factors). This inadequacy is significant for the nodes close to the reflector and minor for the nodes far from the reflector.

The failure of the ADFs to improve the results of the diffusion calculations can be explained by the fact that, as mentioned in the introduction, the ADFs are only approximations to the true discontinuity factors and they do not account for the cell leakage. The same cell leakage is likely to change the average macroscopic cross sections as well. As expected, the difference between the true homogenized parameters and the zero-current ones is larger for the nodes close to the reflector, where leakage is largest.

It follows that, to achieve accuracies of better than 4% in the nodes near the reflector, an improved homogenization method is needed, one that accounts for neutron leakage.

5 REFERENCES

1. K. KOEBKE, “A New Approach to Homogenization and Group Condensation,” Technical Committee Meeting on Homogenization Methods in Reactor Physics, Lugano, Switzerland, (1978)
2. K. SMITH, “Spatial Homogenization Methods for Light Water Reactor Analysis,” Ph.D. thesis, MIT, (1980)
3. K. S. SMITH, “Assembly Homogenization Techniques for Light Water Reactor Analysis”, Progr. Nucl. Energy, 17, 303-335, (1986)
4. S.R. DOUGLAS, “Energy Condensation and Discontinuity Factors”, AECL-8771, 1985
5. G. MARLEAU, A. HEBERT and R. ROY, "A User Guide for DRAGON, Release 3.04", Institut de génie nucléaire, Département de génie mécanique, Ecole Polytechnique de Montréal, (2001)
6. F. LESZCZYNSKI, D. L. ALDAMA, A. TRKOV (EDITORS) "WIMS-D Library Update - Final Report of a Co-ordinated Research Project", IAEA-DOC-DRAFT, (2003)
7. P. J. TURINSKY et al., "NESTLE (V5.2.1) Few-Group Neutron Diffusion Equation Solver Utilizing The Nodal Expansion Method for Eigenvalue, Adjoint, Fixed-Source Steady-State and Transient Problems", Electric Power Research Center, North Carolina State University, Raleigh NC, (2003)
8. P. BOCZAR, "ACR Technology Base: Fuel", Presentation to the US Nuclear Regulatory Commission, (2003)
9. I.C. GAULD, K.A. LITWIN, " Verification and Validation of the ORIGEN-S Code and Nuclear Data Libraries", p30, Scientific Document Distribution Office, AECL, Chalk River, Ontario, Canada, (1995)
10. G. MARLEAU, "Approximate Discontinuity Factor Evaluations in DRAGON", Proceedings of the 24th CNS Annual Conference, Toronto, (2003)